EFFECT OF THE PLY STACKING SEQUENCE ON THE TRANSLAMINAR FRACTURE COHESIVE LAW

Adrián Ortega[1], Pere Maimí[1], Emilio V. González[1], José Ramón Sainz de Aja[2], Federico M. de la Escalera[2]

[1]AMADE, Mechanical Engineering and Industrial Construction Department, Universitat de Girona, Campus Montilivi s/n, Girona, Spain. Email: adrian.ortega@udg.edu Web Page: http://amade.udg.edu
[2]Aernnova Engineering Solutions Ibrica S.A., Structural Integrity Department, 20 Manoteras Avenue Building B, 5th Floor, 28050 Madrid, Spain

Keywords: Cohesive Law, Laminate, Compact Tension, Fracture toughness, Bridging

Abstract

The translaminar fracture of fibre-reinforced composite materials normally develop a large Fracture Process Zone in which fibre bridging and fibre pull-outs take place. This type of fracture is well represented with the use of a Cohesive model, where a fictitious crack grows, capable of transferring closure stresses between the crack surfaces. In the present work, three composite materials have been combined: Carbon fabric, Glass fabric and Unidirectional Carbon tape. In total, 9 hybrid laminates have been combined. Each laminate is made of two materials, while varying the ply stacking sequence and maintaining the in-plane elastic modulus and the laminate thickness constant. With the aid of an algorithm capable of solving the inverse problem, the translaminar cohesive law has been acquired, by fitting experimental load-displacement curves obtained from a fracture test of a Compact Tension specimen. The study concludes with an analysis of the measured cohesive laws, by comparing the effect of the ply stacking sequence of each laminate. The results suggest that placing the Glass fabric plies in the outer faces of the laminate may lead to an increase of the onset and propagation fracture energies.

1. Introduction

Complicated fracture mechanisms take place when a through-the-thickness crack grows in a fibre reinforced composite material. Such inelastic energy dissipation mechanisms may account for matrix cracking, fibre bridging and fibre pull-out. When the energy dissipation mechanisms take place in a relatively large region with respect to the specimen or structure size, Linear Elastic Fracture Mechanics (LEFM) are not applicable, and more sophisticated fracture models such as the Cohesive Zone model [1] are needed. Within the Cohesive Model framework, all the non-linear dissipation mechanisms take place inside a fracture process zone (FPZ), with closure stresses σ_i and crack openings ω_i related by a Cohesive Law (CL), which is generally considered to be a material (or laminate) property.

The use of hybrid materials is of high interest for the science of materials research field as well for industrial applications. These kind of composites may benefit from advantages of each separate material, e.g, improving the damage tolerance, delaying some failure mechanism or even decreasing the total economic cost by using inexpensive materials. The present work focuses on the study of the translaminar cohesive law of hybrid laminates, and how the material of each ply can affect the laminate traction-separation shape. The laminates are made of a combination of two materials: Unidirectional Carbon (UC) tape, woven Carbon fabric (C) and woven Glass fabric (G). For each combination, several stacking

Excerpt from ISBN 978-3-00-053387-7

Table 1: Ply properties of each composite material

Material	E_1 (GPa)	E_2 (GPa)	G_{12} (GPa)	ν_{12}	σ_u (MPa)
C	59.54	54.95	5.21	0.03	804.1
G	19.65	19.24	3.93	0.09	557.8
UC	116.73	8.31	4.67	0.26	1477.1

sequences have been studied, and more concretely, how the location of certain plies can affect the overall translaminar cohesive law.

2. Experimental setup and test specimens

2.1. Materials

Three composite materials have been tested in the experimental campaign: two woven fabrics and an Unidirectional Carbon (UC) tape, the same materials defined in the work of González et al. [2]. The three materials have been supplied by Hexcel®. The fabric materials use HexFlow® RTM 6 mono-component epoxy system. All composites have been supplied with epoxy binders on both sides (with the binder representing about 5% of the total fabric weight). The woven fabrics plies are Carbon (C) fabric type G0926 (5HS, 6K, 370 gsm), and Glass (G) fabric type S2 (style 6781, Z-6040, 303 gsm), while the UC is type G1157 (UD, 6 K, 270 gsm).
The elastic properties of each lamina are found in Table 1. The ply thickness of each material C, G and UC are 0.353 mm, 0.229 mm and 0.247 mm, respectively. The thickness has been obtained from an average of 6 measurements of cured non-hybrid laminates.

2.2. Laminates

The hybrid laminates have been divided in three sets by joining two different materials per laminate: C-G, C-UC and G-UC. The stacking sequences are summarized in Table 2, with the fibre direction of 0^o aligned with the loading direction. In order to achieve a comparative analysis for each set, the ply sequences have been chosen as symmetric, balanced and in-plane quasi-isotropic. The number of plies of each material has also been kept constant. As a result, the in-plane stiffness is constant for each set, although the bending stiffness may vary from laminate to laminate. The C-G laminates are made of $n = 14$ plies, with a cured laminate thickness h of 4.31 mm. In the case of the C-UC laminates $n = 14$ and $h = 4.22$ mm, whereas for the G-UC, $n = 18$ and $h = 4.22$ mm.

2.3. Test configurations

The tests are performed on a CT Specimen Geometry, seen in Fig. 1, with a nominal size of $W = 51$ mm and a pin hole diameter of $d = 8$ mm. The initial crack length is $a_0 = 26$ mm. The tests were carried out following the recommendations by Pinho et al. [3], as no standard procedure has been developed for the determination of the translaminar fracture toughness of fibre-reinforced composite materials using a CT specimen. The test was performed with a screw-driven universal testing machine, loading the specimens at rates of 0.5 mm/min. The crack tip notch was manufactured with a diamond coated disc, ensuring a radius lower than 250 μm, following the recommendations by Laffan et al. [4]. The load cell signal and the extensometer signal were acquired and recorded with a dedicated PC. The displacement was measured with a displacement transducer placed at the crack surface below the load line.

Excerpt from ISBN 978-3-00-053387-7

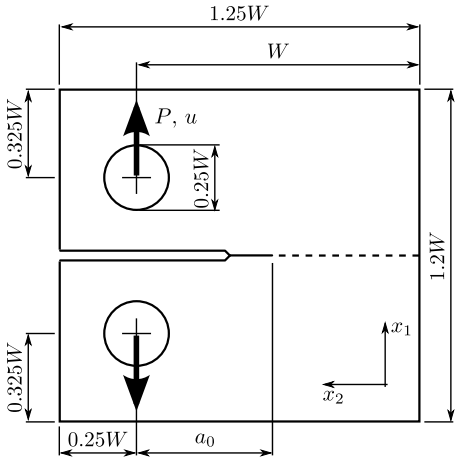

Figure 1: Compact Tension (CT) Specimen Geometry, subjected to a controlled displacement u and measured load P.

Table 2: Hybrid laminates stacking sequences. The 0º direction is aligned with the loading direction.

Materials	Laminates
C-G	L01: $[0^{G}/60^{G}/-60^{G}/(0^{C}/45^{C})_2]_S$
	L02: $[(0^{C}/45^{C})_2/0^{G}/60^{G}/-60^{G}]_S$
	L03: $[0^{G}/(45^{C}/0^{C})_2/60^{G}/-60^{G}]_S$
C-UC	L04: $[0^{UC}/60^{UC}/-60^{UC}/(0^{C}/45^{C})_2]_S$
	L05: $[(0^{C}/45^{C})_2/0^{UC}/60^{UC}/-60^{UC}]_S$
G-UC	L06: $[0^{UC}/45^{UC}/90^{UC}/-45^{UC}/(0^{G}/45^{G})_2/0^{G}]_S$
	L07: $[(0^{G}/45^{G})_2/0^{G}/45^{UC}/0^{UC}/-45^{UC}/90^{UC}]_S$
	L08: $[0^{UC}/45^{UC}/0^{G}/45^{G}/90^{UC}/-45^{UC}/0^{G}/45^{G}/0^{G}]_S$
	L09: $[0^{G}/45^{G}/0^{G}/90^{UC}/-45^{UC}/0^{G}/45^{G}/0^{UC}/45^{UC}]_S$

3. Methodology: Cohesive Zone modelling and inverse problem

The translaminar cohesive law is obtained by means of solving the inverse problem, i.e., determining the cohesive law shape that ensures the predicted u-P curve matches the experimental one. Although the general procedure is hereby briefly presented, the authors highly suggest reading the in-detail procedure published in [5].

3.1. Direct method: Dugdale's condition

A standard CT specimen of size W, shown in Fig. 1, is subjected to the action of a controlled displacement (u) and corresponding load (P) applied at the pin holes. The analytic solution is capable of predicting the FPZ development as a crack grows in pure mode-I along the symmetry plane. The starting point of the problem solution comes from the Dugdale's condition, i.e., the global Stress Intensity Factor (SIF) of the problem, K, must be null [6, 7]:

$$K = K^{P} + K^{\sigma_c} = 0 \tag{1}$$

where K^{P} is the SIF caused by the point load P and K^{σ_c} is the SIF caused by the whole cohesive stress profile σ_c. Although the σ_c is unknown and may change during the FPZ development, it can be

Excerpt from ISBN 978-3-00-053387-7

discretized as a series of small constant stresses of value equal to σ_i applied at the crack surface. The non-linear problem expressed as a superposition of linear problems is shown in Fig. 2.

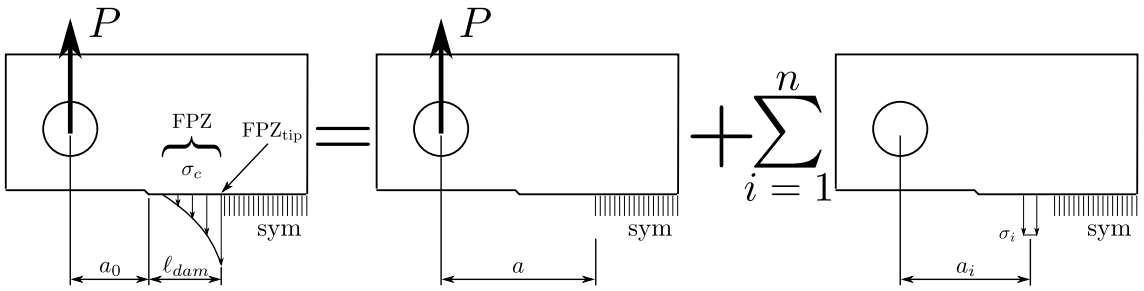

Figure 2: Compact Tension (CT) specimen with a FPZ expressed as a superposition of linear problems.

In order to solve the cohesive stress profile inside the FPZ, the crack opening profile must also be found. It is possible to express the set of openings ω_i as a superposition of the openings caused by each acting load

$$\omega_i = \omega_i^P + \omega_i^{\sigma_c} \tag{2}$$

where ω_i, ω_i^P and $\omega_i^{\sigma_c}$ are the total crack opening, the crack opening caused by the point load P and the crack openings caused by the cohesive stress profile σ_c, respectively.

The solution to the Eq. 2 is obtained from an iterative process, for a given CL. As a result, the stress profile and the crack openings at the FPZ are obtained. Lastly, the load P is obtained by means of Eq. 1, and the displacement u is determined as the crack opening at $a_i = 0$, using again Eq. 2.

3.2. Inverse problem

The inverse problem is solved by means of an algorithm capable of obtaining the CL shape that, when used in conjunction with the direct method, produces a predicted *u-P* curve that matches the experimental data [5].

The algorithm approaches the problem with the following strategy: first, some points from the *u-P* curve are selected around the peak load, while the FPZ is still being developed. These points are used to fit the curve. The length of the Failure Process Zone and the crack tip opening displacements increase as the external displacement is applied. Hence, it is possible to adjust consecutive parts or branches of the Cohesive Law. The algorithm fits first a linear segment of the cohesive law in order to fit the smaller selected displacement of the *u-P* experimental curve. At this moment, the first portion of the CL is found, and its width is determined by the cohesive crack opening at the initial crack tip a_0. The algorithm is continued by adding as many branches as points to be fitted until the whole shape is found.

4. Results and discussion

Fig. 3a shows the *u-P* curve obtained from the Compact Tension fracture test made of the laminate L04. Before fitting the data, a fine Gaussian smoothing has been applied in order to minimize the experimental scatter. The Cohesive Law has been acquired by fitting the points marked with a ∘. Fig. 3b shows the measured CL shape by means of the methodology proposed in Section 3. Observing the shape of traction-separation law, for small crack openings the FPZ is still capable of transferring high stresses. It also features a long tail that transfers low stress levels at larger crack openings. All the studied laminates present a similar behaviour.

Excerpt from ISBN 978-3-00-053387-7

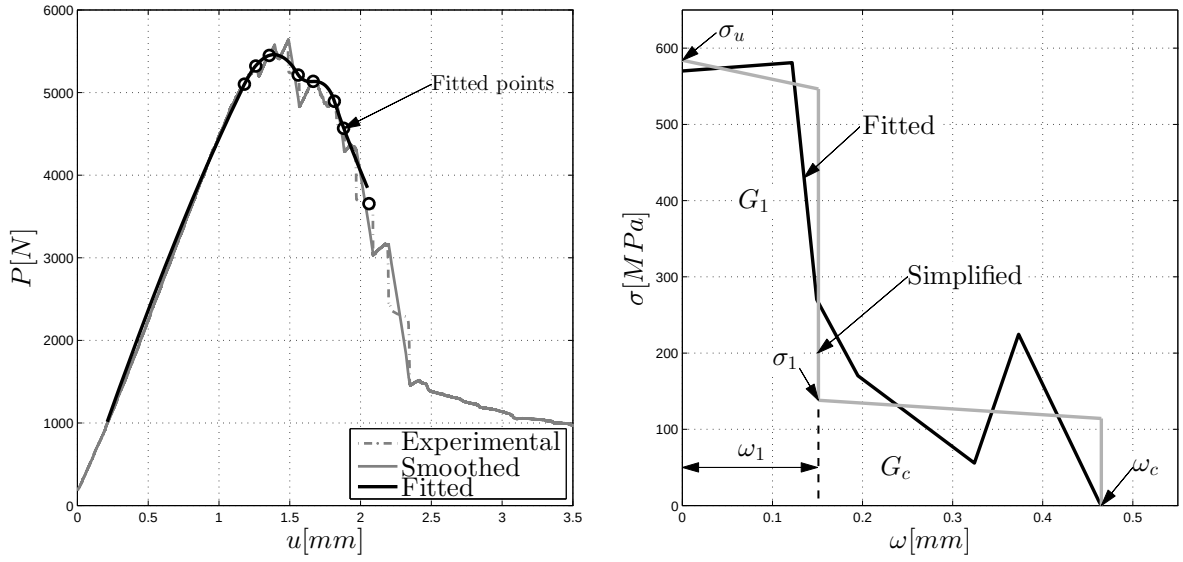

(a) (b)

Figure 3: Laminate L04 (a) experimental load (P) displacement (u) curve, along its respective smoothed and fitted curves. (b) Measured cohesive law and proposed simplified shape.

In order to be able to compare the CL features of each laminate, a simplified cohesive law has been proposed. This simplified shape tries to capture the behaviour described above: the transfer of high stresses at low crack openings and low stress levels for large crack openings. In this manner, the chosen parameters to fully define the CL are : σ_u, σ_1, ω_1, ω_c, G_1 and G_c, shown in Fig 3b. For each measured CL, these parameters have been found by means of a least square fitting.

The found parameters for each laminate can be found in Table 3. With the CL shapes summarized in this manner, it is possible to objectively compare each laminate, and also analyse how the material of the lamina affects the overall laminate tolerance.

Observing the laminates made of Carbon fabric and Glass fabric (C-G), the position of each material has no effect on the onset fracture energy G_1, although the propagation fracture energy G_c values are slightly increased when the Carbon fabric plies are located in the outer faces of the laminate. Moving to the Carbon fabric and Unidirectional Carbon tape laminates (C-UC), placing the UC plies in the outer faces increases the G_c about a 15 %, while placing them in the middle increases G_1 a 15 %. The third group of laminates are the ones made with the most contrasting materials: G and UC. In this case, the effects of the material position on the fracture energy are more evident than in the previous studied laminates. Placing the Glass fabric on the outer faces have a significant effect on both G_c and G_1, with a particular attention to the laminate L07.

5. Conclusion

The translaminar cohesive law has been measured for 9 hybrid laminates. The laminates are divided in three sets, each combining two materials: Unidirectional Carbon tape, woven Carbon fabric and woven Glass fabric. For each set, several ply stacking sequences have been studied, swapping the ply position of each material, while trying to maintain the in-plane elastic modulus and the total laminate thickness as invariant as possible.

A Compact Tension specimen has been tested for each laminate. The translaminar Cohesive Law has

Excerpt from ISBN 978-3-00-053387-7

Table 3: Simplified Cohesive Law parameters for each laminate.

Material	Laminate	G_c [N/mm]	G_1 [N/mm]	ω_1 [mm]	ω_c [mm]
C-G	L01	96.5	70.4	0.174	0.540
	L02	107.9	70.0	0.167	0.385
	L03	92.7	72.7	0.151	0.365
C-UC	L04	125.1	85.5	0.151	0.465
	L05	109.6	98.3	0.169	0.439
G-UC	L06	100.2	86.5	0.174	0.395
	L07	168.8	98.9	0.159	0.533
	L08	90.4	68.0	0.097	0.362
	L09	114.7	82.7	0.159	0.568

been obtained by solving the inverse problem, that is, determining its shape so that the predicted load-displacement curve from the fracture test matches the experimental one. This has been accomplished by an algorithm that fits several experimental points of the load-displacement curve while the Fracture Process Zone is still being developed.

In order to objectively compare all the measured Cohesive Laws, a simplified shape has been proposed. The parameters chosen to compare all the curves are the propagation fracture energy G_c, the onset fracture energy G_1, the crack opening achieved at the first part of the cohesive law ω_1 and the critical crack opening ω_c achieved when the Fracture Process Zone has been totally developed.

From the fracture test and the obtained Cohesive Law shapes, it has been shown that the position of certain materials in the laminate can heavily influence the energy being dissipated during the crack growth. From all the studied combinations, the laminate with a most significant impact on the results are the laminates made of Glass fabric and Unidirectional Carbon tape. The results conclude that allocating the former plies in the outer faces can significantly increase the dissipated energy at lower crack openings G_1, i.e, the onset fracture energy, as well as for the propagation values G_c.

Acknowledgments

This work has been partially funded by the Spanish Government through the *Ministerio de Economa y Competitividad*, under contracts MAT2013-46749-R and MAT2015-69491-C3-1-R.

References

[1] A. Hillerborg, M. Modéer, and P.-E. Petersson. Analysis of crack formation and crack growth in concrete by means of fracture mechanics and finite elements. *Cement and Concrete Research*, 6:773–781, 1976.

[2] E. V. González, P. Maimí, J. R. Sainz de Aja, P. Cruz, and P. P. Camanho. Effects of interply hybridization on the damage resistance and tolerance of composite laminates. *Composite Structures*, 108(0):319–331, 2014.

[3] S. T. Pinho, P. Robinson, and L. Iannucci. Fracture toughness of the tensile and compressive fibre failure modes in laminated composites. *Composites Science and Technology*, 66(13):2069–2079, oct 2006.

Excerpt from ISBN 978-3-00-053387-7

[4] M. J. Laffan, S. T. Pinho, P. Robinson, and A. J. McMillan. Translaminar fracture toughness: The critical notch tip radius of 0 plies in CFRP. *Composites Science and Technology*, 72(1):97–102, dec 2011.

[5] A. Ortega, P. Maimí, Emilio Vicente González, and D. Trias. Characterization of the translaminar fracture cohesive law. *Composites Part A: Applied Science and Manufacturing*, In press, 2016.

[6] D. Dugdale. Yielding of steel sheets containing slits. *Journal of Mechanics Physics of Solids*, 8:100–104, MAY 1960.

[7] G. I. Barenblatt. The Mathematical Theory of Equilibrium Cracks in Brittle Fracture. *Advances In Applied Mechanics*, 7:55–129, 1962.

Excerpt from ISBN 978-3-00-053387-7